Optics & Laser Technology 174 (2024) 110556

Contents lists available at ScienceDirect

Optics and Laser Technology

journal homepage: www.elsevier.com/locate/optlastec

Full length article

Changing the High Strength Steel Surface Properties with Femtosecond Laser Beam

M. Berczeli [a], F. Tajti [a], G. Juhász [a], Z. Weltsch [b,*]

[a] *Department of Innovative Vehicles and Materials, John von Neumann University, Izsáki str. 10, Kecskemét H-6000, Hungary*
[b] *Department of Road and Rail Vehicles, Zalaegerszeg Innovation Park, Széchenyi István University, Egyetem tér 1, Győr H-9026, Hungary*

ARTICLE INFO

Keywords:
Wetting
Surface treatment
Laser
DP600

ABSTRACT

Today, the automotive industry is undergoing rapid change. While manufacturers are constantly switching to fully or semi-electric hybrid models, the weight of the vehicles also increases significantly due to the extra weight of the batteries. Since the weight of vehicles has the most significant influence on their consumption and, with it, harmful emissions (even indirectly far from the place of use), manufacturers strive to keep weight under control with continuous improvements. One of the main directions of the developments is the use of new light but at the same time heavy-duty materials with a wide variety of material combinations. These new material pairings pose challenges to knitting technology solutions, which need to be developed similarly. In the course of our research, we are investigating how the surface properties can be optimized in the case of steel with increased strength for the automotive industry, without additional added material and changes visible to the naked eye. We subject the examined DP600 material to a short-pulse laser beam treatment, and we manage to change the surface structure so that the interface properties measured by wetting are significantly improved. The results are confirmed by electron microscopic examinations.

1. Introduction

In the automotive industry, the greening of reducing consumption and thus emissions, is also emerging [1–3]. One of the most tangible ways to achieve this is through lightweight vehicles. Reducing the curb weight of vehicles significantly reduces the energy demand for propulsion, fuel consumption, and therefore emissions [1,3]. One suitable way to achieve this could be to use high-strength steels and advanced polymer materials in potential applications [4–7]. However, the design of joints between elements with different properties still poses problems and challenges for vehicle manufacturers [8–12].

In our opinion, it is advisable to concentrate on developing a bonding method that can be used on all types of materials at the same time without increasing the mass [13]. One such timely and economical way of non-solvent bonding of different materials is adhesive bonding [14–19]. The higher the surface energy of our material of interest, the higher will be the strength of the adhesion technology applied to the surface. In most cases, the materials used in the modern automotive industry have poor wetting properties [20]. Bonding them in the base state would lead to strength limits and barriers [21]. However, by using the proper preparation and surface treatment process, we can influence the wettability values in a way that is favourable to us [22–24].

The most common and widely used surface energy calculation theory is the Fowkes method [25–28]. By measuring the wetting contact angle and then calculating the Fowkes surface energy, the wetting property of a material can be determined. However, it is expected that this can be varied. This can be achieved by different surface treatment methods. There are emerging technologies that have not yet been widely used for this type of wettability-enhancing surface modification, but have great potential, and are emerging from traditional mechanic-chemical surface treatments, such as plasma and laser beam surface treatment [29,30].

The essence of laser surface treatment is to modify the surface properties - and their variation with layer depth - to achieve the optimum combination of properties required for the technical objective to be achieved, while leaving the properties of the workpiece almost unchanged [31]. In general, the treatment aims is increase the strength and load-bearing capacity of the surface [32] create more favourable friction conditions, improve wear resistance, to increase fatigue resistance by optimizing residual stresses, to increase corrosion resistance, improve cleaning, increase adhesion by using an adhesion technology [33–35].

* Corresponding author.
E-mail addresses: berczeli.miklos@nje.hu (M. Berczeli), weltsch.zoltan@sze.hu (Z. Weltsch).

https://doi.org/10.1016/j.optlastec.2024.110556
Received 25 June 2023; Received in revised form 27 October 2023; Accepted 8 January 2024
Available online 15 January 2024

The use of laser beams as a full mass property modification technology would not be efficient, but it offers an ideal opportunity to achieve highly versatile, highly accurate and productive, well-controlled surface treatment processes [36].

High-energy photons in laser light are always partially absorbed, reflected, or even passed through the material when they meet the substrate [37]. The photons transfer their energy to the top layer of the material, at a depth of about 2 nm, by exciting the atoms and electrons or molecules of the material through their resonance frequency. The energy of the surface treatment can therefore only be transferred to the deeper layers by thermal conduction, which requires high-intensity laser radiation.

In various modern short-pulse surface treatments, the thermal interaction of the laser beam with the workpiece converts the absorbed energy into thermal energy in the material [38]. As a consequence, we can typically speak of the evaporation of the material and finally its transition to a plasma state. In the case of high-energy coupling, the surface heats up, producing first a melt and then a vapour. At sufficiently high energy density levels, plasma can also be formed. By setting the right technological parameters, it is possible to modify only the surface of the material to be treated by the laser beam, leaving the material properties of the array and the deeper parts of the material, the surface aesthetics, intact [39–41].

Based on these considerations, the solid-state modification category of conventional surface treatments and a commonly used procedure to remove unwanted material particles on the surface with a laser beam is laser surface cleaning. As the laser beam reaches the surface, the dirt layer, and typically the oxide layer beneath it, absorbs the energy of the beam. As a result, these layers are completely evaporated and separated from the clean metal or polymer surface. Ultrashort pulse lasers, such as picosecond (ps, 1 ps = 10–12 s), femtosecond (fs, 1 fs = 10–15 s), and attosecond (as, 1 as = 10–18 s) systems. In the case of femtosecond pulsed laser radiation in the matter, a time of a few hundred femtoseconds to a few picoseconds is required for the electrons to equalize their energy. Furthermore, electrons need 1–10 ps to transfer their energy to atoms or ions, which store the excess energy by the amplitude of the motion around the lattice point. This time is much longer than the time it takes for the free electrons to equilibrate in the surface layer. So, the very short pulses only increase the energy of the electrons, heating them, and creating a very hot electron cloud that is not in equilibrium with the crystal lattice because of the large difference in temperature between the two. Due to the short time required, the surface of the material typically changes from solid to plasma state instantaneously during the process and hyper sublimation occurs. In femtosecond pulsed surface treatments, the heat-affected zone is thus very small, leading to more accurate and better machining. The use of ultrashort laser beams opens the possibility of micro- and nano-scale surface modification of various materials, which can be interpreted both in terms of geometry and surface activation [42,43].

In the former case, by increasing the power density of the laser beam, a technology can be achieved whereby the topography of the materials can be modified at will by material removal [44,45]. This technique is laser surface texturing, a widely used method for creating micro- and nano-scale patterns with unique topographical features, which can be applied to almost any material. Laser surface texturing has many advantages over other commonly used mechanical surface texturing methods, such as high dimensional accuracy with an order of magnitude smaller structure size realization, high scanning speed and better repeatability, unlike machining and chemical etching [46–48]. In addition, ultrashort pulse material removal requires no chemicals or other consumables and produces no waste. However, to increase the resolution of the laser beam textured surface modification, it was necessary to reduce the laser beam pulse length, which was reduced to the micro, nano, and femtosecond level through continuous operation. Initially, topographic improvement of surface properties in many materials applications was aimed at improving tribological performance.

Another innovative application of ultrashort laser pulsed surface treatments is their wetting enhancement. Giorano et al. have studied the wettability of titanium and mild steels using ps pulses, testing several different ps lasers where only partial wettability enhancement was achieved [49].

Other studies have investigated the effects on the wetting properties of mild steels using lasers of different wavelengths such as CO_2, Nd:YAG, excimer, and high-power diode lasers [50]. These have achieved improvements in wetting where they have halved the initial wetting contact angle. Hao et al. investigated stainless steel surface treatment where they used bio-grade materials for wetting. With these liquids, they succeeded in achieving a 24° contact angle on stainless steel by ps laser beam surface treatment [51]. Zhao et al. used a pulsed Nd:YAG laser to improve the wetting properties of copper. In their results, the surface energy of copper was improved to 55 mN/m by laser beam treatment an average power of 1500 W and 2000 W. In the best case, the wetting contact angle was reduced from 42° to 31° on the surface treated with a 2000 W laser [52]. Some studies have reported on the improvement of wettability characteristics of Al-Mg alloys by laser treatment, in which Guan et al. determined a significant improvement in the surface energy of laser-melted AZ91D, increasing it from 26 mN/m to 40.7 mN/m in their experiments [53]. Demir et al. studied the wettability of AZ31 magnesium alloy with water. They concluded that increasing the size of the oxidized surface by laser surface treatment allows a decrease in the wetting contact angle [49].

Several authors, such as Ngo and Chun, have proposed in their research a method for the low-temperature annealing of metals to form hydrophobic surfaces [54,55]. This was also observed by Kietzig et al. who found that the formation of a hydrophobic wetting state is related to the change in carbon molecular groups due to the slow decomposition of CO_2 at room temperature [56]. Ngo and Chun supported this theory and showed that low-temperature annealing accelerated this transition due to the more intense decomposition of CO_2 [36,54,55]. Bizi-Bandoki et al. determined that the improvement in wettability could be explained by the appearance of new functional molecular groups. Thus, different heat treatments on the surface achieved wettability-enhancing effects through heat-induced changes in surface molecular groups [57].

Various studies have also been carried out on the application of ultrashort pulses for bonding enhancement. A similar experiment was carried out by Li H and his team, who also performed XPS on the cleaned and modified surfaces, where they found that the cleaning process resulted in a reduction of the oxide layer thickness [58]. L. Hao et al. performed CO_2 laser surface treatment on corrosion-resistant steel and found that the O_2 concentration in the steel interface layer nearly doubled and the surface energy increased by 10% [51]. Indira et al. used an Nd:YAG laser to perform surface treatment on magnesium alloy and studied the effect of this treatment with distilled water. The treatment reduced the contact angle of the distilled water dropped on the surface from 81° to 41° [59]. Giovanna and his team treated DP500 high-strength and AISI 304 corrosion-resistant steel with a transporter laser. They aimed to improve the wetting, with which they achieved an improvement in the shear strength of the bond. In their results, they were able to reduce the untreated 50° wetting edge angle of the substrate to 10°, and with the improvement in wetting, they also experienced an intense roughening of the surface roughness [60].

The effect of changing the surface wetting phenomena on the performance of bonding technologies (expected increase in shear strength), however, the effect of different surface treatments on the surface energy is not sufficiently well understood. Recent advancements in beam technologies are facilitating innovative approaches to modify surface energies, subsequently impacting surface wettability and, in turn, influencing bond strength. Knowledge of the surface energy of radiation technology processes is less studied and therefore there is little reference to the relationship between wetting properties and bond strengths. The uptake of the laser beam processes for surface treatment could be greatly aided if systematic research can demonstrate that the mechanisms of action of the treatments significantly affect the bond strength properties of adhesion bonds through changes in surface energies. Which, in turn, are essential for the uptake of practical applications. The results of the literature survey show that high strength steels have become the materials of choice for modern vehicle structures. On this material, we plan to investigate the effect of laser beam processes on surface energy, the wettability. Accordingly, the research will focus on:

1. Determining laser surface treatment processes based on their mechanism of action with respect to surface energies. To identify the technological data sets that can be used for optimization preparation.
2. To investigate the temporal effects of the time elapsed after the laser beam surface treatments until the formation of bonded joints (environmental effects) on properties important for bonding technology, such as wetting.

2. Material and methods

2.1. Test materials

Among the metals we used for the investigations is DP600-type uncoated steel, which is also widely used as a vehicle body material. Dual Phase steels (DP600) consist of hard martensite islands embedded in soft, malleable ferrite, depending on the desired mechanical properties. In the experiments, we used a 1 mm thick cold rolled DP600 steel plate.

The area of the test specimens was defined as 25×55 mm^2. This is sufficient for surface treatment, wetting, microscopy, and adhesive technology tests. For the surface treatment, wetting and adhesive technology tests, we used a standard geometry that we defined to standardise the experiments. For the DP600 materials, we used a hydraulic board shear to cut them into pieces to completely avoid thermal loading and thus changes in surface texture. The test specimen footprint was defined as 25×55 mm^2. This geometry is suitable for surface treatment, wetting, microscopy, and adhesive technology tests. The plates were cut in such a way that the longest side was parallel to the direction of manufacture and rolling. The edges were sanded by hand with sandpaper to avoid possible damage, preserving the initial surface condition for the experiments. The metal specimens were cleaned immediately before surface treatment with 96% methanol, applied to the surface with sterile cotton wool and wiped. Immediately after cleaning, we dried the materials with a hot air dryer. All material treatments and preliminary surface cleaning were carried out with the maximum effort to ensure the homogeneity of the specimens about each other, so that the actual surface treatment effect could be examined later.

2.2. Ultrafast pulsed femtosecond laser system

For innovative, local laser beam surface treatments, we used a Coherent Monaco 1035 nm laser operating in femtosecond pulse mode (Fig. 1).

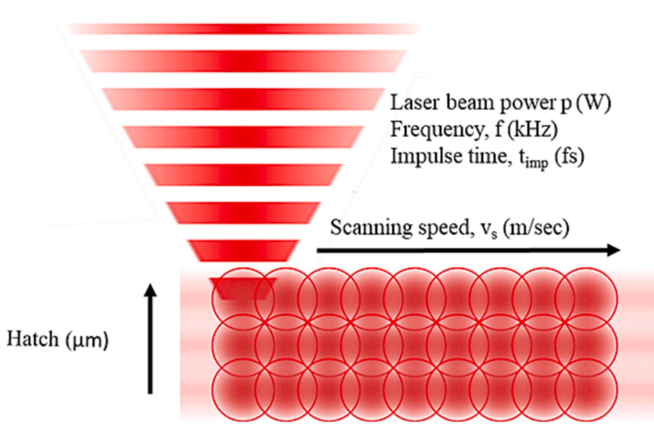

Fig. 1. The strategy and parameters of femtosecond laser scanning.

The machine has a maximum power output of 60 W and a wavelength of 1035 nm. The shortest pulse that can be emitted is 277 fs and the longest is 10,000 fs. The adjustable frequency can be varied from 188 kHz to 50 MHz. The laser beam is guided by mirrors into the scanning head, which uses movable mirrors to direct the laser beam to the desired point. The beam movement is further achieved by a Scanlab F-theta lens scanning optics, the focal spot beam diameter was 80 μm, and the fill was 60 μm.

2.3. Room-temperature droplet method for measuring the contact angle

Immediately after the surface treatment procedures, we measured the wetting contact angle on the specimens using the stilling-drop method. In this method, the droplet does not fall on the surface, so the liquid droplet is not pressed against the surface with a dynamic movement, but only the released liquid is touched to the surface with a slow movement. This gives information on the wettability of the surface and not on how the surface behaves in the face of a drop of liquid falling dynamically on it. The method of measurement is based on a camera and a light source in line with the drop. At the focal point of the measuring system is a stage on which the sample of the surface to be tested is placed. The central axis of the macro lens of the camera coincides with the surface to be tested, so that the plane of the surface as seen in the image and the axis of symmetry of the lens coincide. Above the surface to be examined, there is an automatic pipette with an adjustable height, the axis of which is perpendicular to the surface on which the liquid is placed. In addition, a light source is required which is positioned beyond the object table and illuminated in the direction of the objective, so that the contour of the liquid droplet being examined in profile can be determined on the surface. To perform the measurement, we designed and built the measurement system. Using a micropipette, we used 5 μl droplets for the measurement, which is the most accurate way to record and release the amount of liquid, and similar volume droplets have been used in international literature for measurements after surface treatments. We used two liquids for the droplet measurement to apply the Fowkes method. One liquid was distilled water and the other was ethylene glycol ($C_2H_6O_2$) of >=99% purity. The drop measurements were performed at room temperature 20 ± 1 °C since the polar and dispersive components of the surface tension of water and ethylene glycol are known from literature data at this temperature.

The humidity ranged between 40 and 60%, which is adequate. The polar and dispersive components of distilled water at 20 °C were 51 mN/m and 21.8 mN/m, respectively, and the polar and dispersive components of ethylene glycol at 20 °C were 19 mN/m and 29 mN/m, respectively. The photographs were taken using a Nikon D5300 SLR digital camera. A Tokina AT-X AF 100 mm f/2.8 macro lens was attached to the camera. We set the focal length of the macro lens to the smallest, as this is when the best images are taken with macro lenses and when the focal length is 1:1, which gives the highest magnification. We set the ISO sensitivity range to the lowest, 100. The data we could change was the shutter speed and aperture opening. With the aperture opening, we could control the depth of field, and with the shutter speed, we could control how much light entered the sensor during the taking of the photo. The optimal shooting setting was 1/100th shutter speed and f10 aperture. The measurement procedure for the wetting angle measurement system is as follows: Placing the plate to be measured at the marked position on the measuring system's worktable, placing the pipette tip on the pipette, drawing 5 μl of distilled water into the pipette tip, placing the pipette in the holder, squeezing the water into the tip, lifting the worktable to the drop, returning the worktable to the correct position, photographing the drop after 3 s, replacing the pipette tip, aspirate 5 μl of ethylene glycol into the pipette tip, placing the pipette in the holder, squeezing the ethylene glycol onto the tip, lifting the worktable to the drop, returning the worktable to the correct position, photographing the drop after 3 s, transferring the photographs to the computer, evaluating the photograph using customized perimeter angle measurement software. The resulting photographs were opened in a computer program for measuring perimeters. To measure the drop, first had to take a good quality, sharp photograph of the drop. Then, using a computer, we manually marked the two contact points on the right and left of the liquid droplet and the surface under test. This determined the plane in focus where the liquid droplet profile could be examined and measured. On the photo, we drew in the contacts from the contact point, which should touch the envelope curve of the liquid droplet from the point, and the program then determines the left-hand wetting boundary angle Θ_1 and the right-hand wetting boundary angle Θ_2 by angle measurement. This measurement process is illustrated in Fig. 2.

The most widely used and widely applied surface energy calculation theory is the Fowkes method [28]. The calculation is a two-component model for determining the surface energy of a solid body. Like Owens/Wendt, Fowkes separates the surface energy of a solid into two components. Fowkes' method is mathematically identical to Owens/Wendt's method, but his philosophy is different. Fowkes' method is based on three basic equations that describe the interactions between a solid surface and a fluid.

These three equations are: Young's equation, Dupre's formula for the adhesion energy (1)

$$I_{SL} = \sigma_S + \sigma_L - \sigma_{SL} \tag{1}$$

where: I_SL is the adhesion energy per unit area between the liquid and the solid surface (J/m^2).

The essence of Fowkes' theory is that the adhesion energy between a fluid and a solid surface can be decomposed into the interaction of the dispersive and polar components (9)

$$I_{SL} = 2 \bullet \left[\left(\sigma_L{}^D\right)^{1/2} \bullet \left(\sigma_S{}^D\right)^{1/2} + \left(\sigma_L{}^P\right)^{1/2} \bullet \left(\sigma_S{}^P\right)^{1/2} \right] \tag{2}$$

The combination of these three equations gives the primary equation of the Fowkes method, which we have used most often in our research and which all our surface energy calculation methods refer to (3)

$$\left(\sigma_L{}^D\right)^{1/2} \bullet \left(\sigma_S{}^D\right)^{1/2} + \left(\sigma_L{}^P\right)^{1/2} \bullet \left(\sigma_S{}^P\right)^{1/2} = \frac{\sigma_L \bullet (\cos\theta + 1)}{2} \tag{3}$$

If we divide both sides of the equation, we obtain the primary equation of the Owens/Wendt method, which proves the mathematical equality between the two methods.

The Fowkes method typically uses the boundary angle values of two fluids. One fluid that has only a polar component and one fluid that has both a disperse and a polar component. It is recommended to use a liquid with only a polar component in the resting drop method for boundary angle measurements because it simplifies the primary formula to the following formula (4)

$$\sigma_S{}^D = \frac{\sigma_L \bullet (\cos\theta + 1)^2}{4} \tag{4}$$

This allows the dispersive component of the solid surface to be determined directly, from which the total surface tension can be calculated by substituting the determined values back into Eq. (3). The recommended test fluids are diiodomethane and distilled water. It should be noted that international literature and research groups use the unit mN/m for the determination of surface energy, whereas the Hungarian language would prefer to refer to J/m^2 for surface energy, but these are equivalent units.

In their research, Siddaiah et al. tested whether the method could be used with two liquids that have both polar and disperse components, only to solve a system of two unknown equations. The Fowkes method is often used for adhesion and coating problems, as Fowkes' equation is suitable for calculating the adhesion energy between adhesive and surface or coating and surface [61]. The fact that according to Fowkes, a polar component can only interact with a polar component predicts that the surface and adhesive adhesion energy will be at its maximum when the surface tension components are polar and dispersive in similar percentages between the surface and adhesive.

2.4. Scanning electron microscopy investigations

We used scanning electron microscopy (SEM) to investigate the topography-changing ability of surface treatments. The SEM equipment used for the studies were Zeiss Sigma 300 Gemini FESEM and Tescan MIRA 3 SEM systems. In the case of the Zeiss equipment, an InLens SE detector was used, with an accelerating voltage of 10 kV, in high vacuum mode, with an aperture of 30 µm, the working distance in this case being 3 mm. The images were taken at a resolution of 2048x1536 at a scanning speed of 8. In the case of the tescan device, an In-Beam SE detector was

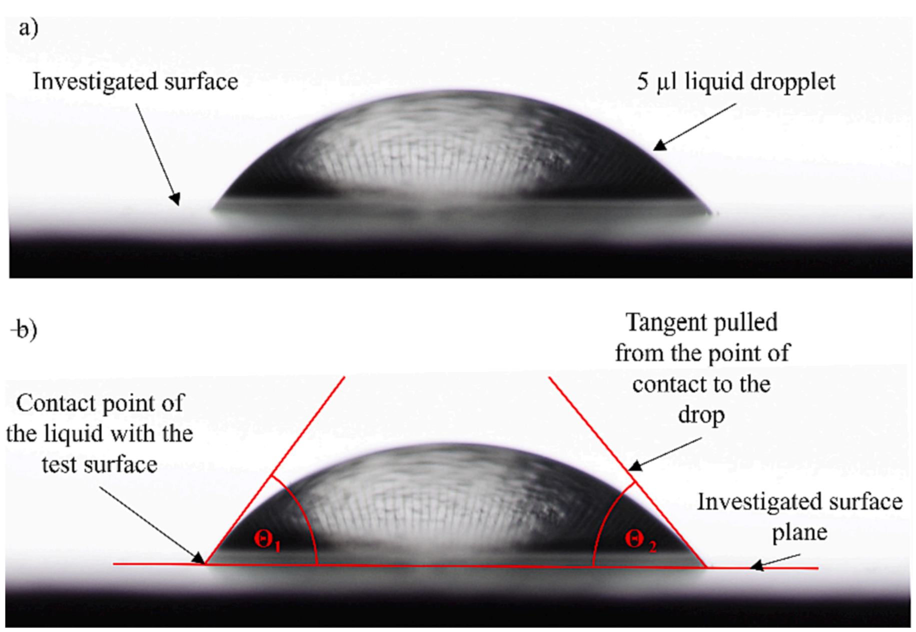

Fig. 2. The process of measuring the contact angle of a drop of liquid placed on a surface: a): the position of the droplet of liquid placed on the surface, b): the process of evaluating the contact angle measurement, determination of theta degree.

used with an accelerating voltage of 5 kV in high vacuum mode and a working distance of 5 mm. The images were taken at a resolution of 1536 × 1716.

2.5. Measurement method

We used a femtosecond pulsed laser for irradiation, taking advantage of the short pulse laser beam's ability to change the surface due to the high-power density of the pulses striking the surface. By testing the process data and controlling the location and number of pulses, we aim to create a hydrophilic surface.

During the wetting tests, we treated the surface of a 25 × 55 mm^2 steel plate with different settings. We treated each specimen with different process data and after treatment, we investigated its wetting properties by measuring the contact angle with water and with ethylene glycol. In the preliminary tests, a total of 4 different scanning speeds were tested in the range of 0.5 m/min−2400 m/min.

3. Results

In the experiments, we found that at very low speeds up to about 120 m/min scanning speed, too much heat is introduced into the sample, causing the surface to discolour and burn. At higher speeds of 600–2400 m/min, the wetting properties improve, but banding is observed on the surface, which is because the acceleration and deceleration of the Galvo motors moving the mirrors in the scanning optics are not uniform due to the high speed. Based on preliminary experience, a scanning speed of 300 m/min was chosen as a starting point. Based on these results, the experimental data range for femtosecond laser alignment is shown in Table 1.

Preliminary tests showed a significant improvement in wettability and no visible lesions on the surface. The diameter of the laser beam on the scanned surface was 80 μm. The laser beam source was applied at 188 kHz, with a pulse width of 300 fs and a step size of 60 μm to ensure proper filling of the treated surface.

The variable process data was the average power of the pulsed laser beam, which was measured at high resolution from 0 to a maximum of 60 W. I performed the wetting tests on the modified surfaces, the results are shown in Fig. 3.

Using the measured boundary angles, we calculated the energy change in the boundary surface due to each treatment based on Fowkes' equation system (Fig. 4). The values measured on the untreated surface are marked with a horizontal line.

Fig. 4 shows that the total surface energy increases as the laser beam power increases. Compared to an untreated surface energy of 26 mN/m, the energy of a plate treated above an average power of 10 W increases to 85 mN/m. With the treatment, the interfacial energy was increased by a factor of almost four, which is expected to have a positive effect on the wetting capacity of the adhesive.

Based on the trend of the results in Figs. 3 and 4, it is possible to divide the surface wetting changes caused by the different power pulses into 4 stages. In the first stage, up to an average power of 7.5 W, the wetting angle does not change much, the reason being that in this case the even lower power laser beam only scans the surface and performs a surface cleaning, which removes residual dirt, dust, etc. To get an explanation of the processes that take place on the surface other than the surface cleaning and the improvement of the wetting characteristics, we took SEM images of the treated and untreated test pieces. Fig. 5 shows the macro topography of the treated and untreated surfaces. This image was taken at an average treatment power of 7.5 W.

It can be seen in the SEM image that the untreated, inhomogeneous surface in the upper left half is completely changed by the femtosecond pulsed surface treatment. The macro topography of the surface has become more homogeneous, and the surface uniformity is visible.

The image was taken in backscattered electron mode so that the contrast of the image is caused by different element numbers. From these results, it can be concluded that the laser beam creates a cleaned and homogeneous surface layer since the difference between the two areas is the disappearance of the dark parts.

Examining the surface from the same view, but in secondary imaging mode, results in the lesion shown in Fig. 6.

The clear appearance of the surface treatment bands can be seen in the SEM image compared to the base materials. At this magnification, it is possible to visualise the conditions of overlapping of the scan lines caused by the lower power surface treatment. This alone is sufficient for a slight improvement in wetting.

In stage 2, after an average power of 7.5 W, the surface starts to change and there is a significant, large improvement in surface wetting. In stage 3, this wetting increases further until the hydrophilic state is reached, from an average power of 10.5 W onwards, plasma bursts appear on the surface during the treatment, due to the peak power due to the high average power and the peak power condensed to a short pulse duration, which means a power of the order of Megawatts for the small spot diameter. These plasma bursts also affect the surrounding, already treated surface, resulting in a simultaneous change in surface micro-topography, surface activation and cleaning. We have successfully achieved a hydrophilic state, while no drastic topographical changes can be detected on the surface by the eye. In the 3rd wetting step, we tested the areal extent of 0.5 μl of distilled water to find the optimal wetting direction. Similar to the previous test procedure, we prepared areas treated with different femtosecond laser beam averaging powers on the surface of the alcohol-cleaned steel plate, with the largest spreading area examined by dropping the droplets in the middle. This was done under the criterion that no severe surface changes affecting aesthetics should be induced by the laser beam treatment. Thus, when examining the small amount of liquid, the area treated at an average power of 51 W showed the greatest spreading of water. In a further phase of the experiment, this was determined to be the optimum wetting process data for the DP600 steel femtosecond pulsed laser. In this good wetting condition, only a small surface change, hardly noticeable to the eye, occurred on the steel test specimen, which was the aim of our research. The surface treatment of the sample at an average power of 51 W is shown in Fig. 7.

At higher average power, a larger area of the 80 μm laser spot reaches the power intensity limit where the incident pulse already affects the surface. It is possible to see the degree of overlap and the laser beam spot

Table 1
Constant and variable data for femtosecond laser beam surface treatment technology.

	Relative speed of movement between laser beam and workpiece, v_s (m/min)
	300
Average power of the laser beam for the tested speed of movement, P_{avg} (W)	1.5
	3
	4.5
	6
	7.5
	7.8
	8.1
	8.4
	8.7
	9
	9.3
	9.6
	9.9
	10.2
	10.5
	10.8
	11.4
	12
	13.5
	15
	16
	increments by 4 up to 60

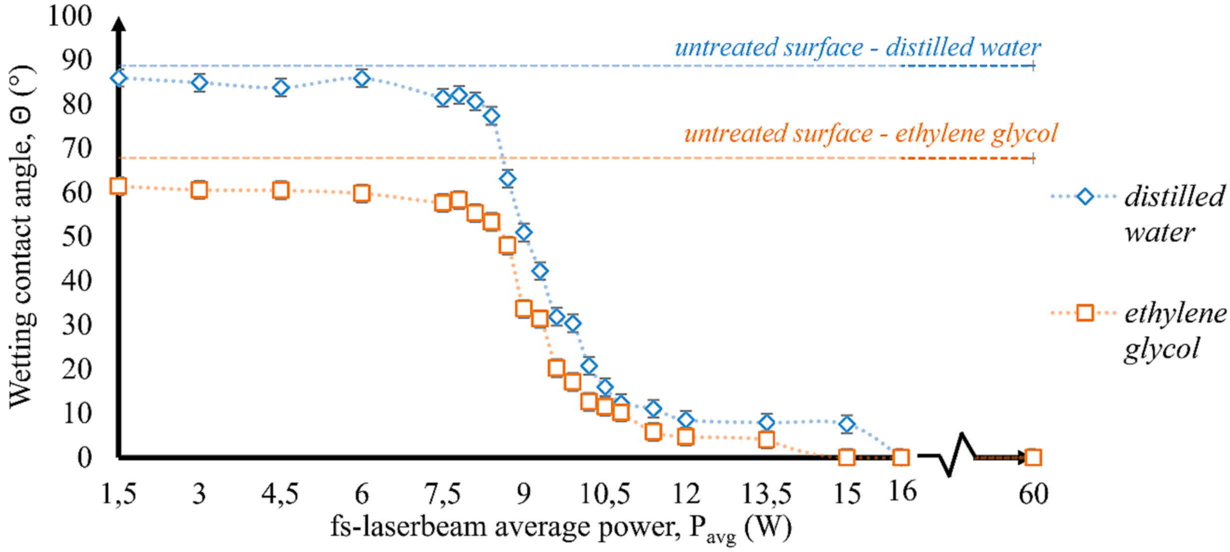

Fig. 3. Changing of wetting contact angle depending on the fs-laserbeam average power using distilled water and ethylene glycol.

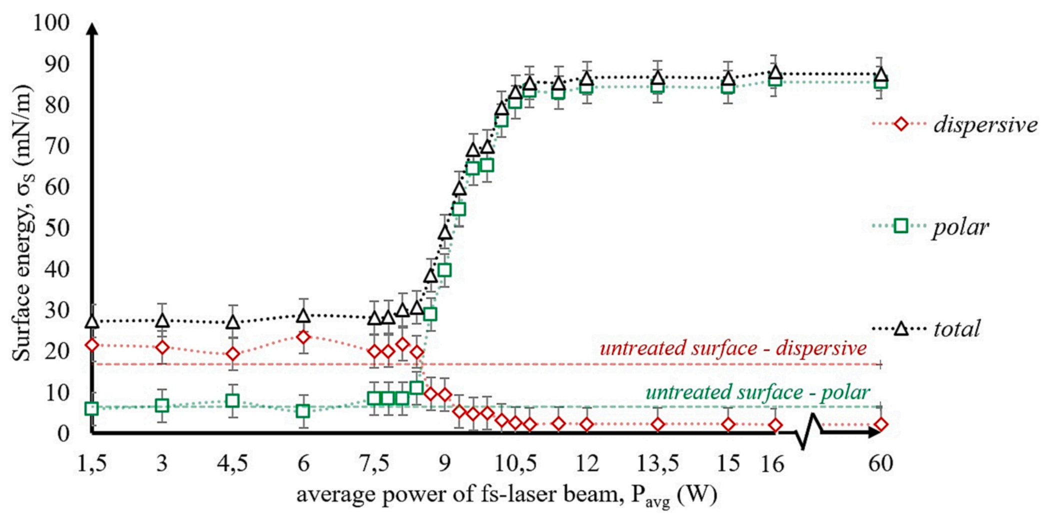

Fig. 4. Polar, dispersive and total surface energy on DP600 steel as a result of femtosecond laser beam surface treatment.

propagation along the edge of the treated surface compared to the surface topography of the substrate. The figure shows that (ignoring the paragraph, runout band) compared to the inhomogeneous structure of the untreated substrate shown in the top left half, the laser beam has created a trace, microstructure on the surface per pulse. The periodicity of the surface is determined by the successive impact and overlap of the pulses on the surface. A higher magnification of the homogeneous treated area taken from the centre is shown in Fig. 8.

Observe in the SE detector image that the surface is made up of regularly repeating pulse traces. The regularity of the pulses concerning each other is influenced by the scanning speed and the degree of filling. The reason for the dark ellipsoidal spots seen in the image is that the laser beam power was at its maximum here, so the surface may have been slightly melted by the plasma explosion during the removal of the overlying layer. The ellipsoidal shape is due to the polarisation of the laser beam exiting the beam source, where the electric and magnetic waves make the light linearly polarised, and this is the reason for the shape. What is striking is that the bright bands seen in the image have formed in areas of lower power intensity and can already be seen in the image to contain microstructure. For samples surface-treated at the optimal average power of 51 W, the amount and homogeneity of the microstructures in the white band in the previous figure are increased, as can be seen in Fig. 9 from the BSE detector.

In this case, as the laser beam power increased, a larger area of apparently more homogeneous periodicity was created, which can be seen in the right half of the image, while in comparison the untreated surface of the base material can be seen on the left. However, the ellipse traces shown in Fig. 8 are still visible in the image, but their frequency has changed.

The laser surface treatment shows that some of the micro-strain on the rolled surface of the base material has been removed and homogenised, while the larger 25–30 μm spots have not been removed. Since the surface was already hydrophilic in this range, the surface deformation shown in the figure is also the reason for the good wettability of the surface, and since the treatment was carried out in the air, the surface could react with the air during the laser treatment and thus the hydrophilic state could be created.

SE imaging images of the specific surface structure within the electron column with increasing magnification are shown in Fig. 10.

The Fig. 10 shows the repetitive structure created on the surface by a femtosecond pulsed laser, called LIPSS (Laser-induced periodic surface structure). DP600 steel surface by irradiation with a linearly polarized

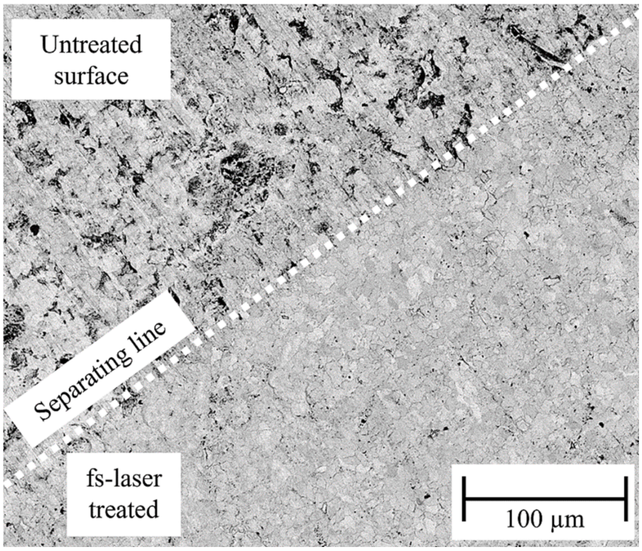

Fig. 5. Surface cleaning effect of untreated and fs-laser beam treated surface structure for the 7.5 W treatment.

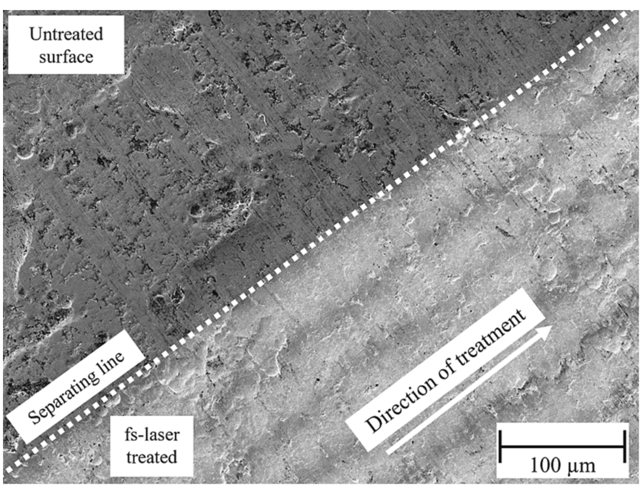

Fig. 6. Surface modification effect of fs-laser treatment bands, paths for 7.5 W treatment.

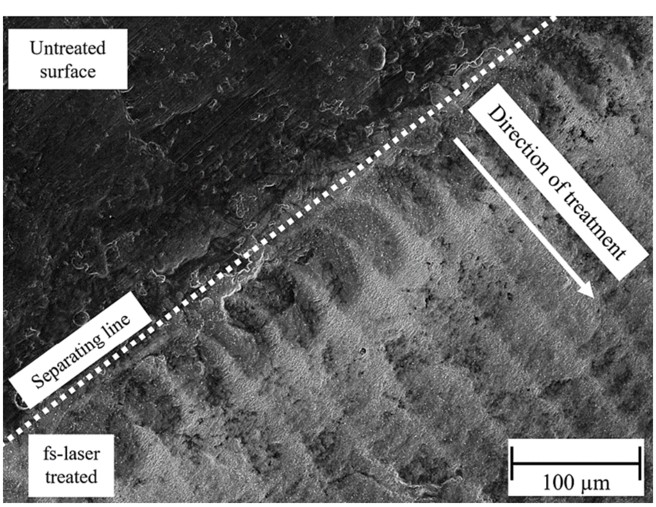

Fig. 7. SEM image of the topography-altering effect of femtosecond individual pulses on DP600 steel at an average power of 51 W.

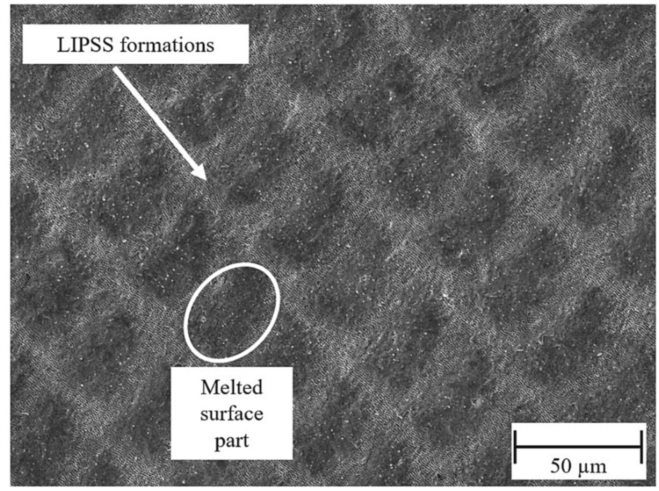

Fig. 8. Using an average power of 51 W, periodically repeating structures, LIPSS were formed locally on the surface when the pulses were superimposed.

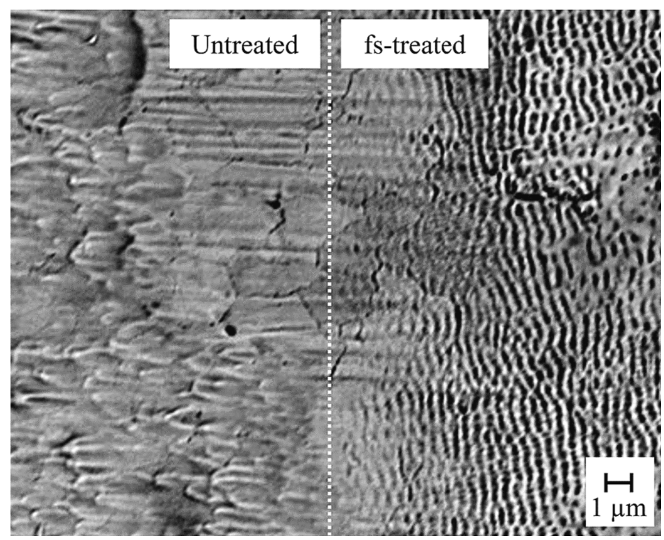

Fig. 9. Laser Induced Periodic Surface Structure on the DP600 steel surface at an average power of 51 W due to femtosecond pulses.

femtosecond laser beam at a power close to the melting threshold and is formed as a microstructure of the surface topography. As the average power of the femtosecond laser beam varied during the study, it is clear that the extent of the LIPSS generated on the surface also varied. The spatial arrangement and periodicity of this microstructure are typically smaller than the wavelength of the femtosecond laser beam used, as can be seen from the scale of the plots, since the equipment used emits light at a wavelength of 1035 nm, while the SEM images show a smaller periodicity. The periodicity of the LIPSS generated in our research work with the current technology parameters is based on the periodicity of a low spatial frequency LIPSS (Low-Spatial Frequency LIPPS - LSFL). The most widely accepted theory to explain LSFL formation is based on the interference of incident laser radiation with surface electromagnetic waves that are generated by scattering from the surface. The structure formed by LSFL is typically perpendicular to the polarization of the laser beam. This can be seen in Fig. 9 and 10, as the LSFLs are formed perpendicular to the linearly polarized ellipses formed by the laser beam spots, which are traced by the pulses on the DP600 steel. This nanometre-scale conformational accuracy greatly increases the bonding surface area ratio of the DP600 steel, which provides additional adhesion surface area.

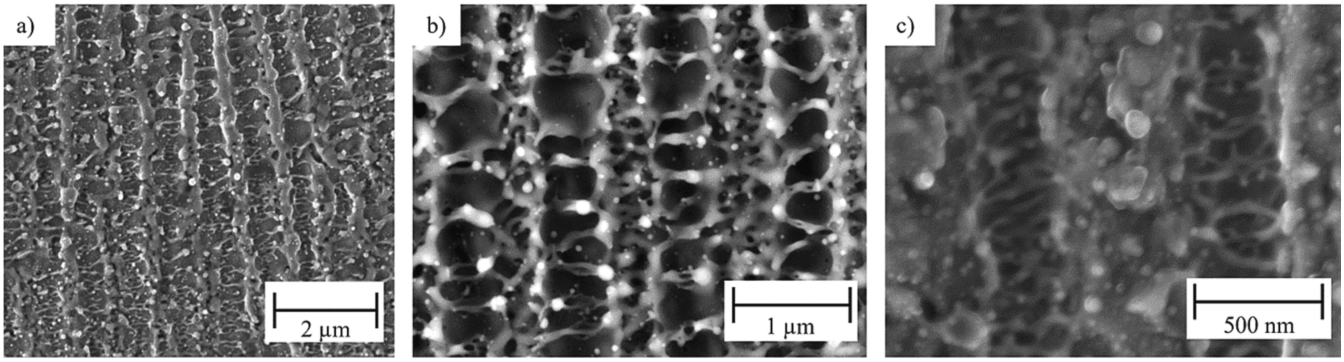

Fig. 10. LIPSS formation on DP600 steel at different magnifications: a) group of LIPSS formation, b) four periods of LIPSS, c) longitudinal and cross forming of LIPSS.

In stage 4, with an average power of 55 W, the surface treatment was converted to surface ablation and a high level of the substrate was introduced into the plasma state due to hyper sublimation. Note that the wetting also remained hydrophilic because of this, but the surface roughness and the material bands removed from the surface changed the macro topography of the DP600 steel to a large extent, which was an undesirable process (Fig. 11).

The results show that it was possible to improve the wettability properties with femtosecond laser beams. The trend of the results shows that by increasing the amount of energy input, the wetting properties of the DP600 steel plate can be improved.

The highest energy level achievable by the quiescent drop method and the Fowkes method was met by the femtosecond laser beam surface treatment, so this method can be considered effective in improving the surface energy of DP600 steel without macroscopic topography changes and any visible aesthetic changes. In a good wetting condition, 3 mechanisms are involved, first, the energy of the laser beam in pulses cleans the surface, bringing all the grains into a plasma state, and then at a certain level a specific microtopographic lesion is produced by the pulses, secondly, during the laser beam-material interaction, a thin layer of the material is immediately converted into a plasma state and a small plasma explosion occurs on the surface during the treatment at the point of pulse impact, accompanied by light and sound, so that it can be easily detected. And in a third mechanism, the resulting plasma beam may be able to affect the activation of interfacial molecules.

Fig. 12 shows that the water is fully spread over the surface for 30 min and reaches the 20° contact angle in about 45 min. However, gradually over time, the good wetting condition is lost. Again, this can be due to two things, one is the deposition of dust and particles in the air on the surface and the other is the activated surface reacting with the air and thus gradually losing its functionality.

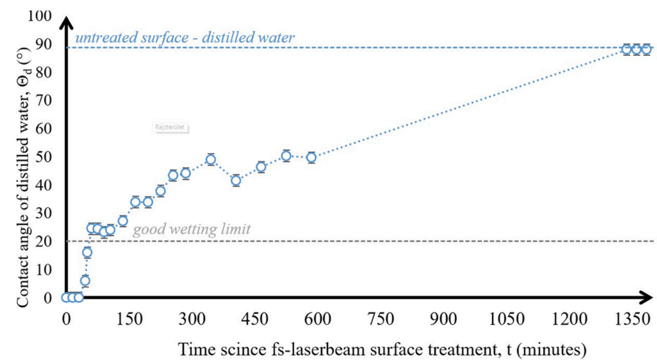

Fig. 12. Change in the wetting angle of hydrophilic DP600 steel as a function of time.

By comparing our results on DP600 steel with those of other researchers, we can say that by using femtosecond lasers, we have established the topographical and wetting cause of the changes produced by the laser beam on the surface with a higher parameter resolution and a more detailed series of experiments.

Thus, the causes of the light-matter interaction processes have been explored to a greater extent. Furthermore, in a great deal of research, research groups only investigate the interfacial energy altered by the laser beam and do not consider its correlation and applicability in an adhesion technology such as bonding.

4. Conclusions

We treated a DP600 type steel plate with an ultrashort pulse laser

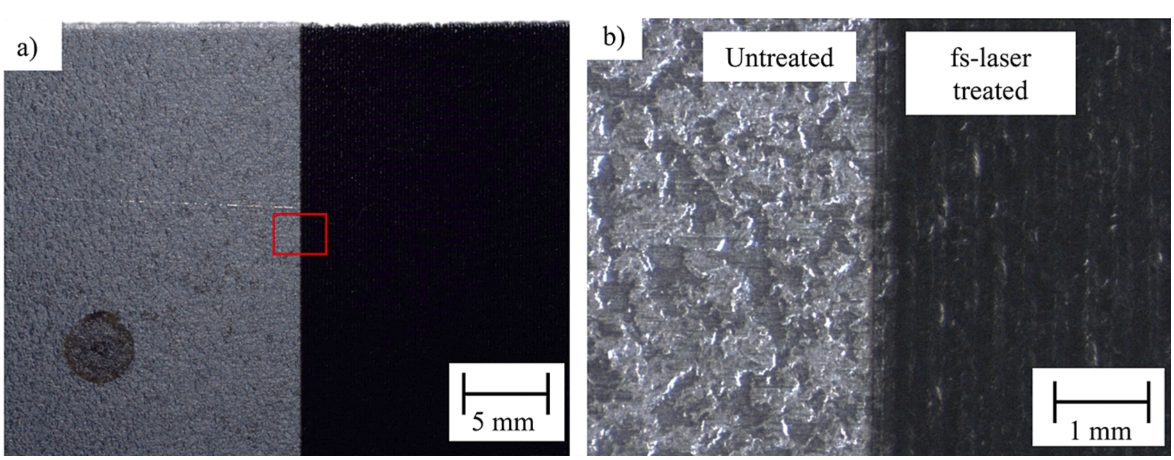

Fig. 11. Ablation on the steel surface of a DP600 treated with an average power of 55 W: a) macro and b) micro images.

beam.

We examined how the wetting ability of the material changes as a result of the laser treatment. We determined the dispersed and polar components as well as the total surface energies. Based on the performance of the laser, we divided the results into four different stages. A significant wetting improvement starts at a power greater than 7.5 W, with a power greater than 9 W we speak of good wetting, while with a power greater than 16 W, perfect wetting is achieved for both processed liquids.

The treated samples were subjected to scanning electron microscopy and the following findings were made. The macro topography of the sample changes because of the laser treatment. Treatment with lower power (7.5 W) results in a homogeneous clean surface. As a result of high-performance treatment, a repetitive surface structure is formed, which we identified as LIPSS. It is clear from the results that the LIPSS formed on the surface significantly changes the interface properties without any visible changes occurring with the naked eye. We established the optimum process data to achieve hydrophilicity without aesthetic degradation using a laser beam with a wavelength of 1035 nm, a diameter of 80 μm, a scanning speed of 300 m/min, a fill of 60 μm, a repetition rate of 188 kHz, impulse time of 300 fs and an average power of 51 W. The bond strength of adhesive bonding technologies can be optimized with the method without the use of activating chemicals.

Their experimental results proved that femtosecond laser beam surface treatment is a suitable solution for creating optimal interface conditions. By changing the treatment parameters, it was even possible to create a completely hydrophilic surface, which demonstrates the potential inherent in the technology.

We managed to implement the interface change in such a way that there was no change visible to the naked eye on the surface. With SEM images, it was possible to prove that the nanostructure formed on the treated surface has a significant effect on the process.

The tested technology may be suitable for application in vehicle industry bonding technology areas, as evidenced by the time-dependent tests.

Declaration of Competing Interest

The authors declare that they have no known competing financial interests or personal relationships that could have appeared to influence the work reported in this paper.

Data availability

No data was used for the research described in the article.

Acknowledgements

Project no. RRF-2.3.1-21-2022-00009, titled National Laboratory for Renewable Energy has been implemented with the support provided by the Recovery and Resilience Facility of the European Union within the framework of Programme Széchenyi Plan Plus.

This work was supported by the Janos Bolyai Research Scholarship of the Hungarian Academy of Sciences (ZW).

References

[1] A. Peppas, K. Kollias, D.A. Dragatogiannis, C.A. Charitidis, Sustainability analysis of aluminium hot forming and quenching technology for lightweight vehicles manufacturing, Int. J. Thermofluids. 10 (2021) 100082, https://doi.org/10.1016/J.IJFT.2021.100082.

[2] X. Meng, J. Xu, W. Liang, Z. Xu, K.C. Li, A lightweight anonymous cross-regional mutual authentication scheme using blockchain technology for internet of vehicles, Comput. Electr. Eng. 95 (2021) 107431, https://doi.org/10.1016/J.COMPELECENG.2021.107431.

[3] D. He, V.K. Soo, H.C. Kim, M. Doolan, Life Cycle Primary Energy Demand and Greenhouse Gas Emission benefits of vehicle lightweighting with recycled carbon fibre, Proc. CIRP 98 (2021) 43–48, https://doi.org/10.1016/J.PROCIR.2021.01.003.

[4] E. Sahraei, K. Digges, D. Marzougui, K. Roddis, High strength steels, stiffness of vehicle front-end structure, and risk of injury to rear seat occupants, Accid. Anal. Prev. 66 (2014) 43–54, https://doi.org/10.1016/J.AAP.2014.01.004.

[5] S. Baek, J. Song, H. Lee, S. Park, K.-H. Song, S. Lee, S.-J. Lee, C. Chen, D. Kim, Robust bonding and microstructure behavior of aluminum/high-strength steel lap joints using resistance element welding process for lightweight vehicles: experimental and numerical investigation, Mater. Sci. Eng. A (2021) 142378, https://doi.org/10.1016/J.MSEA.2021.142378.

[6] Y. Chang, Z.H. Meng, L. Ying, X.D. Li, N. Ma, P. Hu, Influence of hot press forming techniques on properties of vehicle high strength steels, J. Iron Steel Res. Int. 18 (2011) 59–63, https://doi.org/10.1016/S1006-706X(11)60066-6.

[7] N. Wang, Y. Li, L. xiu Du, D. Wu, X. hua Liu, Fatigue property of low cost and high strength wheel steel for commercial vehicle, J. Iron Steel Res. Int. 16 (2009) 44–77, https://doi.org/10.1016/S1006-706X(09)60059-5.

[8] A.M. Sadoun, F.A. El-Wadoud, A. Fathy, A.M. Kabeel, A.A. Megahed, Effect of through-the-thickness position of aluminum wire mesh on the mechanical properties of GFRP/Al hybrid composites, J. Mater. Res. Technol. 15 (2021) 500–510, https://doi.org/10.1016/J.JMRT.2021.08.026.

[9] F. Lambiase, M. Durante, A. Di Ilio, Fast joining of aluminum sheets with Glass Fiber Reinforced Polymer (GFRP) by mechanical clinching, J. Mater. Process. Technol. 236 (2016) 241–251, https://doi.org/10.1016/J.JMATPROTEC.2016.04.030.

[10] M. Hakamada, T. Furuta, Y. Chino, Y. Chen, H. Kusuda, M. Mabuchi, Life cycle inventory study on magnesium alloy substitution in vehicles, Energy 32 (2007) 1352–1360, https://doi.org/10.1016/J.ENERGY.2006.10.020.

[11] D. Kumar, R.K. Phanden, L. Thakur, A review on environment friendly and lightweight Magnesium-Based metal matrix composites and alloys, Mater. Today:. Proc. 38 (2021) 359–364, https://doi.org/10.1016/J.MATPR.2020.07.424.

[12] A. Hassani, S.R. Safavi, V. Hosseini, A comparison of light-duty vehicles' high emitters fractions obtained from an emission remote sensing campaign and emission inspection program for policy recommendation, Environ. Pollut. 286 (2021) 117396, https://doi.org/10.1016/J.ENVPOL.2021.117396.

[13] G.J. Béres, Z. Lukács, M. Tisza, Springback evaluation of Tailor Welded Blanks at V-die bending made of DP Steels, Proc. Manuf. 47 (2020), https://doi.org/10.1016/j.promfg.2020.04.266, 1366-1373 PG–8.

[14] J.H. Back, J.U. Hwang, Y.H. Lee, D. Baek, J.W. Park, H.J. Kim, J.H. Kim, H.K. Song, M.J. Yoo, Morphological study and mechanical property of epoxy-foam adhesives based on epoxy composites for automotive applications, Int. J. Adhes. Adhes. 87 (2018) 124–129, https://doi.org/10.1016/J.IJADHADH.2018.09.010.

[15] R. Ciardiello, Mechanical characterization and separation tests of a thermoplastic reinforced adhesive used for automotive applications, Proc. Struct. Integr. 24 (2019) 155–166, https://doi.org/10.1016/J.PROSTR.2020.02.014.

[16] M. Alfano, C. Morano, F. Moroni, F. Musiari, G. Danilo Spennacchio, D. Di Lonardo, Fracture toughness of structural adhesives for the automotive industry, Proc. Struct. Integr. 8 (2018) 561–565, https://doi.org/10.1016/J.PROSTR.2017.12.055.

[17] M.D. Banea, M. Rosioara, R.J.C. Carbas, L.F.M. da Silva, Multi-material adhesive joints for automotive industry, Compos. B Eng. 151 (2018) 71–77, https://doi.org/10.1016/J.COMPOSITESB.2018.06.009.

[18] S.I. Ao, International Association of Engineers, World Congress on Engineering : WCE 2012 : 4–6 July, 2012, Imperial College London, London, U.K., (2012) 2065.

[19] S. Maláková, A. Guzanová, P. Frankovský, V. Neumann, E. Janoško, Glued joints in the automotive industry, Acta Mech. 4 (2019) 23–28, https://doi.org/10.22306/AM.V4I4.53.

[20] Z.F. Kovács, Z.J. Viharos, J. Kodácsy, Surface flatness and roughness evolution after magnetic assisted ball burnishing of magnetizable and non-magnetizable materials, Measurement 158 (2020) 107750.

[21] F. z, I. Hren, Welding opportunities of al-based composites reinforced with ceramic particles, Perner's Contacts. 19 (2019) 101–107 PG–7. https://m2.mtmt.hu/api/publication/30693987.

[22] E. Arzt, H. Quan, R.M. McMeeking, R. Hensel, Functional surface microstructures inspired by nature – From adhesion and wetting principles to sustainable new devices, Prog. Mater Sci. 120 (2021) 100823, https://doi.org/10.1016/J.PMATSCI.2021.100823.

[23] L.K. Koopal, Wetting of Solid Surfaces: fundamentals and Charge effects, Adv. Colloid Interface Sci. 179–182 (2012) 29–42, https://doi.org/10.1016/J.CIS.2012.06.009.

[24] J.H. Lee, J. Park, M.H. Myung, M.J. Baek, H.S. Kim, D.W. Lee, Stretchable and recoverable acrylate-based pressure sensitive adhesives with high adhesion performance, optical clarity, and metal corrosion resistance, Chem. Eng. J. 406 (2021) 126800, https://doi.org/10.1016/J.CEJ.2020.126800.

[25] D.Y. Kwok, D. Li, A.W. Neumann, Fowkes' surface tension component approach revisited, Colloids Surf. A Physicochem. Eng. Asp. 89 (1994) 181–191, https://doi.org/10.1016/0927-7757(94)80117-7.

[26] E. Matykina, I. Garcia, J.J. De Damborenea, M.A. Arenas, Comparative determination of TiO2 surface free energies for adhesive bonding application, Int. J. Adhes. Adhes. 31 (2011) 832–839, https://doi.org/10.1016/j.ijadhadh.2011.08.003.

[27] S. Natsui, K. Tonya, H. Nogami, T. Kikuchi, R.O. Suzuki, SPH simulations of binary droplet deformation considering the Fowkes theory, Chem. Eng. Sci. 229 (2021), https://doi.org/10.1016/J.CES.2020.116035.

[28] F.M. Fowkes, Determination of interfacial tensions, contact angles, and dispersion forces in surfaces by assuming additivity of intermolecular interactions in surfaces, J. Phys. Chem. 66 (2002) 382, https://doi.org/10.1021/J100808A524.

[29] C.K. Akkan, M. Hammadeh, S. Brück, H.W. Park, M. Veith, H. Abdul-Khaliq, C. Aktas, Plasma and short pulse laser treatment of medical grade PEEK surfaces for controlled wetting, Mater. Lett. 109 (2013) 261–264, https://doi.org/10.1016/j.matlet.2013.07.030.

[30] R. Kromer, S. Costil, C. Verdy, S. Gojon, H. Liao, Laser surface texturing to enhance adhesion bond strength of spray coatings – Cold spraying, wire-arc spraying, and atmospheric plasma spraying, Surf. Coat. Technol. 352 (2018) 642–653, https://doi.org/10.1016/j.surfcoat.2017.05.007.

[31] K. Kun, J. Líska, Z. Weltsch, Replication of microstructures formed by femtosecond laser during injection moulding, in: S. Chattopadhyaya, G.M. Krolczyk, F. Pude, D. Klichová, S. Hloch (Eds.), Advances in Manufacturing Engineering and Materials II, Springer International Publishing, 2021, pp. 11–290, https://doi.org/10.1007/978-3-030-71956-2_24.

[32] K. Kun, P. Boza, Investigation of inserts surface structures on injection moulded parts, IOP Conf. Ser. Mater. Sci. Eng. 448 (2018), https://doi.org/10.1088/1757-899X/448/1/012052.

[33] S.P. Hu, C.N. Niu, H. Bian, X.G. Song, J. Cao, D.Y. Tang, Surface-activation assisted brazing of Al-Zn-Mg-Cu alloy: improvement in microstructure and mechanical properties, Mater. Lett. 218 (2018) 86–89, https://doi.org/10.1016/j.matlet.2018.01.153.

[34] Z. Yang, Y.L. Tian, C.J. Yang, F.J. Wang, X.P. Liu, Modification of wetting property of Inconel 718 surface by nanosecond laser texturing, Appl. Surf. Sci. 414 (2017) 313–324, https://doi.org/10.1016/j.apsusc.2017.04.050.

[35] A. Rudawska, Adhesive properties of metals and metal alloys, Surf. Energy (2015), https://doi.org/10.5772/60599.

[36] C.V. Ngo, D.M. Chun, Effect of heat treatment temperature on the wettability transition from hydrophilic to superhydrophobic on laser-ablated metallic surfaces, Adv. Eng. Mater. 20 (2018) 1701086, https://doi.org/10.1002/ADEM.201701086.

[37] B. Jaroslav, J. Štěpán, B. Libor, K. Ladislav, G.J. Béres, Metallurgy of the weld joints on the weldox 1100 steel realised with the laser hybrid technology, Perner's Contacts 2 (2019) 11–66. https://m2.mtmt.hu/api/publication/30693760.

[38] A.W. Alshaer, L. Li, A. Mistry, The effects of short pulse laser surface cleaning on porosity formation and reduction in laser welding of aluminium alloy for automotive component manufacture, Undefined. 64 (2014) 162–171, https://doi.org/10.1016/J.OPTLASTEC.2014.05.010.

[39] H. Shin, D. Kim, Cutting thin glass by femtosecond laser ablation, Opt. Laser Technol. 102 (2018) 1–11, https://doi.org/10.1016/j.optlastec.2017.12.020.

[40] X.C. Wang, H.Y. Zheng, P.L. Chu, J.L. Tan, K.M. Teh, T. Liu, B.C.Y. Ang, G.H. Tay, High quality femtosecond laser cutting of alumina substrates, Opt. Lasers Eng. 48 (2010) 657–663, https://doi.org/10.1016/j.optlaseng.2010.02.001.

[41] L.C. Tshabalala, C.P. Ntuli, J.C. Fwamba, P. Popoola, S.L. Pityana, Surface texturing of sialon ceramic by femtosecond pulsed laser, Proc. Manuf. 7 (2017) 660–667, https://doi.org/10.1016/j.promfg.2016.12.098.

[42] K. Yin, H. Du, Z. Luo, X. Dong, J.A. Duan, Multifunctional micro/nano-patterned PTFE near-superamphiphobic surfaces achieved by a femtosecond laser, Surf. Coat. Technol. 345 (2018) 53–60, https://doi.org/10.1016/j.surfcoat.2018.04.010.

[43] H. Zhou, C. Li, Z. Zhou, R. Cao, Y. Chen, S. Zhang, G. Wang, S. Xiao, Z. Li, P. Xiao, Femtosecond laser-induced periodic surface microstructure on dental zirconia ceramic, Mater. Lett. 229 (2018) 74–77, https://doi.org/10.1016/j.matlet.2018.06.059.

[44] G.V. Kuznetsov, D.V. Feoktistov, E.G. Orlova, K. Batishcheva, S.S. Ilenok, Unification of the textures formed on aluminum after laser treatment, Appl. Surf. Sci. 469 (2019) 974–982, https://doi.org/10.1016/j.apsusc.2018.11.046.

[45] D. Bhaduri, A. Batal, S.S. Dimov, Z. Zhang, H. Dong, M. Fallqvist, R. M'Saoubi, On design and tribological behaviour of laser textured surfaces, Proc. CIRP 60 (2017) 20–25, https://doi.org/10.1016/J.PROCIR.2017.02.050.

[46] H. Chen, J. Peng, L. Fu, X. Wang, Y. Xie, Solder wetting behavior enhancement via laser-textured surface microcosmic topography, Appl. Surf. Sci. 368 (2016) 208–215, https://doi.org/10.1016/j.apsusc.2016.01.167.

[47] V.D. Ta, A. Dunn, T.J. Wasley, J. Li, R.W. Kay, J. Stringer, P.J. Smith, E. Esenturk, C. Connaughton, J.D. Shephard, Laser textured superhydrophobic surfaces and their applications for homogeneous spot deposition, Appl. Surf. Sci. 365 (2016) 153–159, https://doi.org/10.1016/j.apsusc.2016.01.019.

[48] D.V. Ta, A. Dunn, T.J. Wasley, R.W. Kay, J. Stringer, P.J. Smith, C. Connaughton, J. D. Shephard, Nanosecond laser textured superhydrophobic metallic surfaces and their chemical sensing applications, Appl. Surf. Sci. 357 (2015) 248–254, https://doi.org/10.1016/j.apsusc.2015.09.027.

[49] G. Menci, A.G. Demir, D.G. Waugh, J. Lawrence, B. Previtali, Laser surface texturing of β-Ti alloy for orthopaedics: effect of different wavelengths and pulse durations, Appl. Surf. Sci. 489 (2019) 175–186, https://doi.org/10.1016/J.APSUSC.2019.05.111.

[50] K.Y. Benyounis, A.G. Olabi, M.S.J. Hashmi, Multi-response optimization of CO2 laser-welding process of austenitic stainless steel, Opt. Laser Technol. 40 (2008) 76–87, https://doi.org/10.1016/j.optlastec.2007.03.009.

[51] L. Hao, J. Lawrence, Y.F. Phua, K.S. Chian, G.C. Lim, H.Y. Zheng, Enhanced human osteoblast cell adhesion and proliferation on 316 LS stainless steel by means of CO2 laser surface treatment, J. Biomed. Mater. Res. B Appl. Biomater. 73 (2005) 148–156, https://doi.org/10.1002/JBM.B.30194.

[52] Z. Zhao, C. Wang, M. Li, L. Wang, L. Kong, The effects of pulsed Nd:YAG laser irradiation on surface energy of copper, Appl. Surf. Sci. 252 (2006) 4257–4263, https://doi.org/10.1016/J.APSUSC.2005.07.005.

[53] Y.C. Guan, W. Zhou, H.Y. Zheng, Z.L. Li, Solidification microstructure of AZ91D Mg alloy after laser surface melting, Appl. Phys. A 2010 101:2. 101 (2010) 339–344, doi: 10.1007/S00339-010-5880-0.

[54] C.V. Ngo, D.M. Chun, Control of laser-ablated aluminum surface wettability to superhydrophobic or superhydrophilic through simple heat treatment or water boiling post-processing, Appl. Surf. Sci. 435 (2018) 974–982, https://doi.org/10.1016/j.apsusc.2017.11.185.

[55] C.V. Ngo, D.M. Chun, Fast wettability transition from hydrophilic to superhydrophobic laser-textured stainless steel surfaces under low-temperature annealing, Appl. Surf. Sci. 409 (2017) 232–240, https://doi.org/10.1016/j.apsusc.2017.03.038.

[56] A.-M. Kietzig, J. Lehr, L. Matus, F. Liang, Laser-induced patterns on metals and polymers for biomimetic surface engineering, Laser Appl. Microelectr. Optoelectr. Manuf. (LAMOM) XIX 8967 (2014) 896705, https://doi.org/10.1117/12.2042894.

[57] P. Bizi-Bandoki, S. Valette, E. Audouard, S. Benayoun, Time dependency of the hydrophilicity and hydrophobicity of metallic alloys subjected to femtosecond laser irradiations, Appl. Surf. Sci. 273 (2013) 399–407, https://doi.org/10.1016/J.APSUSC.2013.02.054.

[58] H. Li, A. Belkind, F. Jansen, Z. Orban, An in situ XPS study of oxygen plasma cleaning of aluminum surfaces, Surf. Coat. Technol. 92 (1997) 171–177, https://doi.org/10.1016/S0257-8972(97)00079-0.

[59] K. Indira, C. Sylvie, W. Zhongke, Z. Hongyu, Investigation of wettability properties of laser surface modified rare earth Mg alloy, Proc. Eng. 141 (2016) 63–69, https://doi.org/10.1016/j.proeng.2015.08.1106.

[60] G. Rotella, M. Alfano, T. Schiefer, I. Jansen, Enhancement of static strength and long term durability of steel/epoxy joints through a fiber laser surface pre-treatment, Int. J. Adhes. Adhes. 63 (2015) 87–95, https://doi.org/10.1016/j.ijadhadh.2015.08.009.

[61] A. Siddaiah, B. Mao, A.K. Kasar, Y. Liao, P.L. Menezes, Influence of laser shock peening on the surface energy and tribocorrosion properties of an AZ31B Mg alloy, Wear 462–463 (2020) 203490, https://doi.org/10.1016/j.wear.2020.203490.